Design and implementation of Control System based on DSP and FPGA for Magnetically suspended Control Moment Gyro

Zhang yang[a], Liu kun[a], Feng jian[a], Wei jingbo[b], Zhang zhizhou[a]

[a] National University of Defense Technology, Deya Street 109, Changsha, China, zy_nudt@foxmail.com
[b] Naval University of Engineering, Jiefang Street 717, Wuhan, China

***Abstract*—In order to implement the high stability and low vibration suspension control of magnetically suspended control moment gyro (MSCMG). This article describes the design and implementation of control system based on digital signal processor (DSP) and field programmable able gate array (FPGA) for MSCMG. The controller takes DSP as the master controller to perform the core control algorithms such as decentralized PID control, cross feedback control and adaptive notch control. The FPGA as a coprocessor for data acquisition of the 6-channel displacement and current, the speed measurement of the gimbal servo system and high-speed rotor, the generating of the three-level pulse width modulation (PWM) and the timing planning of the whole control system. Performance testing results are proved the validity of the proposed control system based on the MSCMG prototype system. Experiment results show that the maximum radial position error at the rotation speeds of 3000 rpm /min is less than 5% of the protection gap.**

I. INTRODUCTION

Supported by the magnetic bearing, MSCMG has many advantages such as no friction, high precision, long life and extremely small vibration and so on, which is the ideal inertia actuator for spacecraft attitude control systems such as the space station and the agile satellite [1-3]. The magnetic bearing controller is the core of the magnetic bearing control system, and its control performance will directly affect the performance indicators of the whole system.

Magnetic bearing controller includes controller and power amplifier. The controller mainly realizes the functions such as acquisition of rotor displacement, realization of control algorithm, output current command and so on. The power amplifier then makes the coil current track the controller's desired current according to the controller's instructions. The control of MSCMG needs to implement some control algorithm such as four-axis decentralized control for stable suspension, cross feedback control for suppressing gyroscopic effect[4], and unbalance compensation for overcoming the synchronous vibration that caused by the imbalance of rotor quality[5]. The power amplifier needs to realize the current control algorithm and pulse width modulation of the power switch drive signal.

The early simulation controller is inconvenient to debug, it is difficult to implement more complex control algorithms, and it can't meet the high-precision control requirements of the MSCMG. The digital controller is easy to debug because its control algorithm is implemented by software, and it is easy to add other function expansion algorithms such as vibration control. Therefore, the performance of the magnetic bearing can be well improved.

At present, the core processor of the magnetic bearing controller has two solutions: DSP and FPGA. Moreover, the controller and power amplifier are designed separately using two processors. In recent years, more and more controllers use DSP+FPGA architecture [6-9]. The DSP is mainly responsible for implementing the algorithm as the computing core, and the FPGA as the auxiliary processor is responsible for signal acquisition, preprocessing, and communications.

The architecture has strong computational capabilities and flexible interfaces. It is the development trend of magnetic levitation controllers in the future.

In this paper, a six-channel and five-freedom magnetic bearing controller is designed using a DSP+FPGA architecture, and the performance test results of the controller are given.

II. DYNAMIC MODEL OF THE ROTOR OF MSCMG

The MSCMG studied in this paper is supported by six magnetic bearings. Two radial magnetic bearings are used to realize the translational control of radial two-degrees-of-freedom. Four axial magnetic bearings are used to realize the translational control of axial single-degree-of-freedom and the revolve control of three-degrees-of-freedom around the radial direction. The revolve control of single-degree-of-freedom around the axial direction is driven by brushless DC motor. The rotor dynamics model is shown in Fig 1.

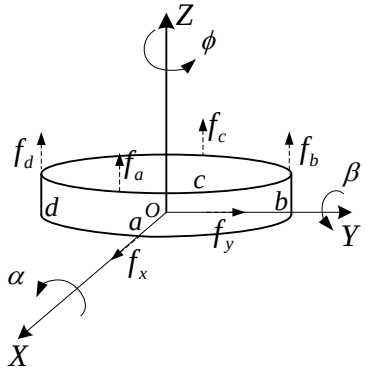

Figure 1. The rotor dynamics model of MSCMG

The O-XYZ is the body coordinate system attached to the rotor. ϕ is the rotation angle of the rotor, which is driven by motor. α and β are the deflection angles of the rotor along the X-axis and Y-axis of the body coordinate system, respectively.

The radial motion equations of the magnetic bearing rotor are as follows:

$$\begin{cases} m\ddot{x} = f_x + F_{dx} \\ m\ddot{y} = f_y + F_{dy} \end{cases} \quad (1)$$

Where, m is the mass of the rotor. x and y are the radial relative displacement of the center of mass of the rotor in the X axis and Y axis. f_x and f_y are the force of magnetic bearing in the X axis and Y axis. f_{dx} and f_{dy} are the disturbing force such as rotor static unbalance and so on in the X axis and Y axis.

The axial motion equation of the magnetic bearing rotor are as follows:

$$\begin{cases} m\ddot{z} = f_a + f_b + f_c + f_d + F_{dz} \\ J_d\ddot{\alpha} + J_p\Omega\dot{\beta} = r(f_b - f_d) + M_{dx} \\ J_d\ddot{\beta} - J_p\Omega\dot{\alpha} = r(f_c - f_a) + M_{dy} \end{cases} \quad (2)$$

Where, z is the axial relative displacement of the center of mass of the rotor in the Z axis. f_a, f_b, f_c and f_d are the control force of four axial magnetic bearings. F_{dz} is the disturbing force in the Z axis. J_d is the rotational inertia that the rotor around the radial. J_p is the rotational inertia that the rotor around the axial. $\Omega = \dot{\phi}$ is the rotational speed of the rotor. M_{dx} and M_{dy} are the component of the X-axis and Y-axis of disturbing torque that caused by the unbalance of the rotor. r is the distance between the center of mass of the rotor and the point of action of the electromagnetic force.

III. THE STRUCTURE OF THE CONTROL SYSTEM

As shown in Fig. 2, the magnetic bearing control system of MSCMG consists of two parts: controller and power amplifier.

The controller will collect the displacement signal from the six-channel displacement sensor, and then output the six-channel current instruction through the operation of the control algorithm such as six-channels decentralized PID control algorithm, cross feedback control algorithm and adaptive notch compensation algorithm.

According to the control signal given by the controller, the power amplifier realizes the tracking of the coil current to the instruction current through the three-level PWM modulation strategy, and then generates the electromagnetic force to realize the stable suspension of the flywheel rotor.

IV. FUNCTIONAL DESIGN OF DSP

The digital controller uses a high performance 32-bit floating-point DSP chip TMS320C6713B with powerful computing power. The main program of DSP and the flow diagram of interrupt service are shown in Fig. 3.

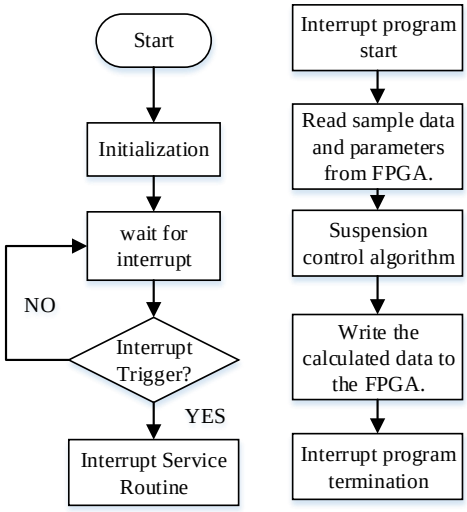

Figure 3. The main program of DSP and the flow diagram of interrupt service

The calculation frequency of the displacement ring and current ring is 6.67KHZ and 20KHZ respectively.

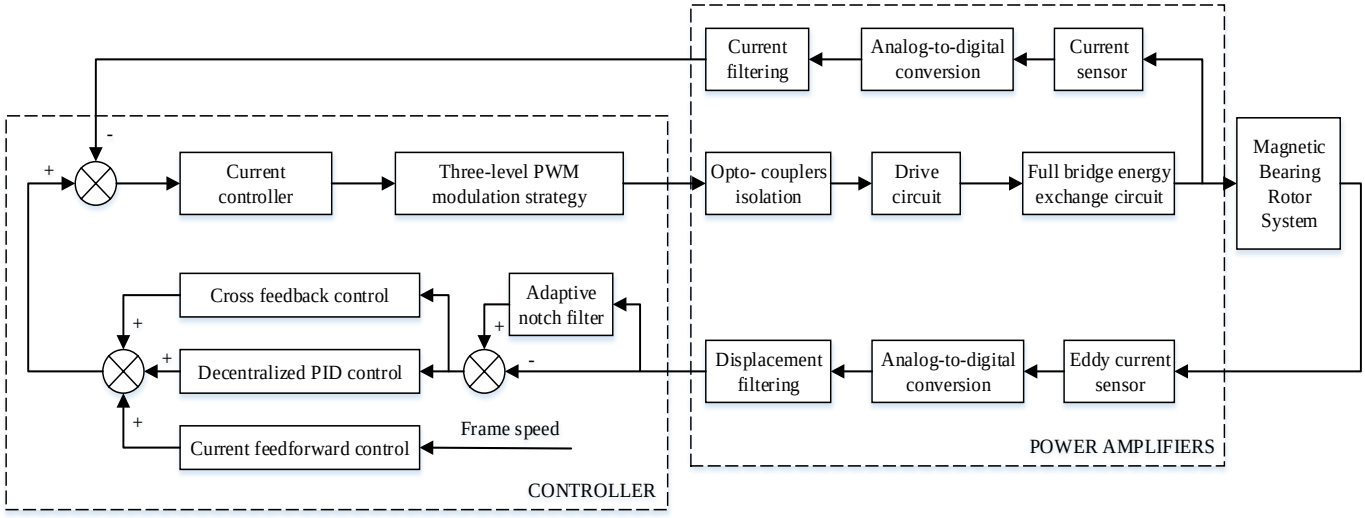

Figure 2. The structure of magnetic bearing control system of MSCMG

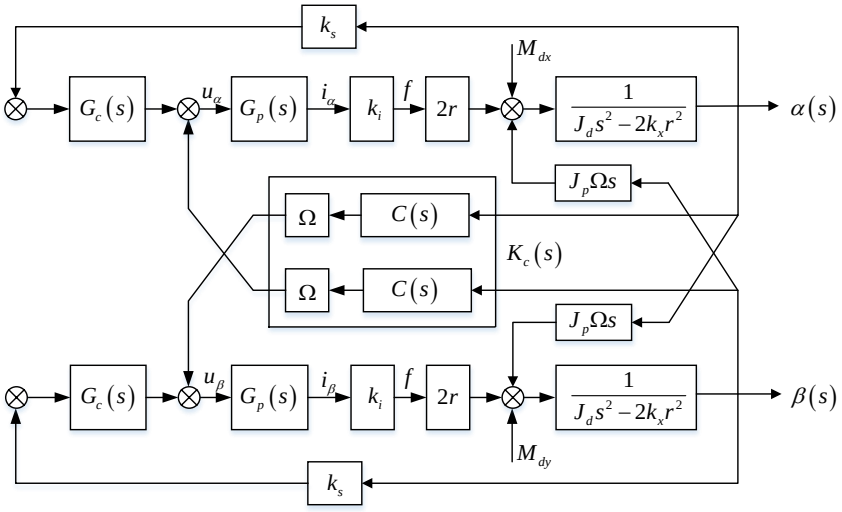

Figure 4. The control block diagram of PID control and cross feedback control

A. Decentralized PID control and cross feedback control

FIG. 4 shows the control structure diagram of the inclined control channel.

$G_c(s)$ is the transfer function of the axial tilt-channel controller. $G_p(s)$ is the transfer function of the power amplifier. $C(s)$ is the transfer function of cross feedback controller. k_s is the sensitivity coefficient of the displacement sensor. k_x and k_i are the displacement stiffness coefficient and the current stiffness coefficient of the hybrid magnetic bearing respectively.

The transfer function of PID controller and cross feedback controller is respectively taken as:

$$G_c(s) = K_p(1 + \frac{1}{\tau_i s} + \tau_d s) \tag{3}$$

$$C(s) = k_1 - k_2 \frac{T_r s}{1 + T_r s} = \frac{k_1(1 - bT_r s)}{1 + T_r s} \tag{4}$$

To discretize equation (3) and equation (4)

$$G_c(k) = K_p e(k) + K_i \sum_{j=0}^{k} e(j) + K_d[e(k) - e(k-1)] \tag{5}$$

$$C(k) = \frac{\frac{k_1 \alpha(k)}{T_s + 2bT_r} + \frac{k_1 \alpha(k-1)}{T_s - 2bT_r} - \frac{c(k-1)}{T_s - 2T_r}}{T_s + 2T_r} \tag{6}$$

Where, $b = k_2 / k_1 - 1$.

B. Adaptive notch filter

Adaptive notch filter is used to suppress the synchronous current caused by unbalance vibration. In order to realize active vibration control of magnetic bearing rotor.

It is inserted in parallel in the signal path and multiplied by a factor ε, and then it is different from the input $u(t)$ to get the output signal $y(t)$. It will become an adaptive synchronous notch filter and its structure is shown in Fig. 5.

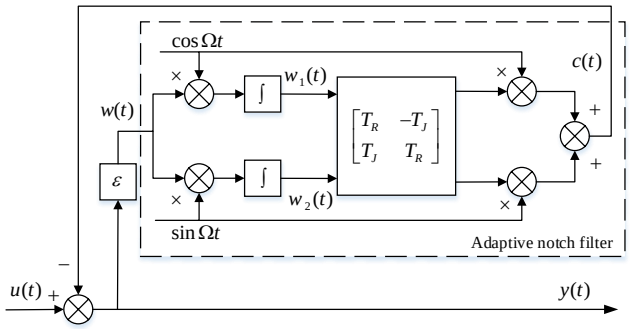

Figure 5. The schematic of adaptive notch filter

The input and output relations of the adaptive notch filter in the time domain can be expressed as

$$c(t) = \begin{bmatrix} \cos \Omega t & \sin \Omega t \end{bmatrix} \begin{bmatrix} T_R & -T_J \\ T_J & -T_R \end{bmatrix} \int \begin{bmatrix} \cos \Omega t \\ \sin \Omega t \end{bmatrix} w(t)\, dt \tag{7}$$

Find the derivation of equation (5)

$$\ddot{c}(t) + \Omega^2 c(t) = T_R \dot{w}(t) - \Omega T_J w(T) \tag{8}$$

After the Laplace transform, the transfer function can be expressed as

$$\frac{c(s)}{w(s)} = \frac{T_R s - T_J \Omega}{s^2 + \Omega^2} \tag{9}$$

According to Equation (9) and Fig.5, the transfer function of the adaptive synchronous notch filter can be expressed as

$$\frac{y(s)}{u(s)} = \frac{s^2 + \Omega^2}{s^2 + \Omega^2 + \varepsilon(T_R s - T_J \Omega)} \tag{10}$$

The adaptive synchronous notch filter is a band-stop filter in essence and it's open-loop gain to the synchronous signal is 0 and for other frequency signals is 1. And that It does not distort the phase of the signal. When it connects to the feedback control loop, the system will not respond to the synchronous signal in the external input and eliminate the synchronous signal in the control current.

V. FUNCTIONAL DESIGN OF FPGA

The FPGA mainly completes the controller parameter setting, current and displacement data sampling and AD conversion as the coprocessor. Before the calculation, the sample data needs to be preprocessed by FPGA, and after the calculation, the calculation results need to be read by FPGA. It would generate waveform of three-level PWM, and control the power tube of full bridge converter circuit based on the voltage instruction. The block diagram of control circuit is shown in the Fig. 6.

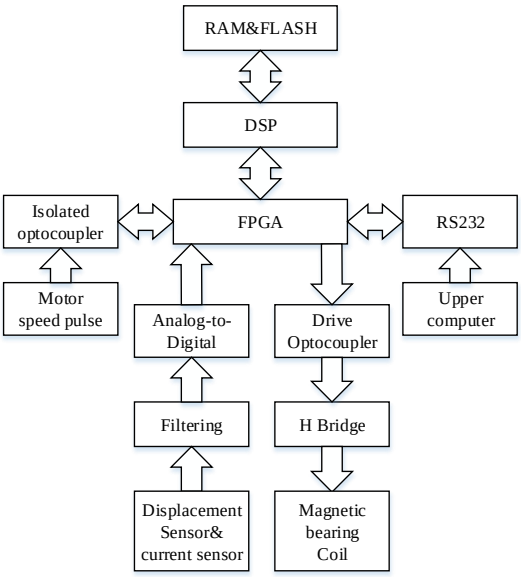

Figure 6. The block diagram of control circuit based on DSP+FPGA

A. *Design of three level PWM module.*

The three-level PWM module is mainly composed of triangle wave generator and comparator. The triangular wave generator counts up from the zero initial state, reaches the set maximum count value, starts to count down in the opposite direction, and counts up to zero and then starts to count up. This cycle forms a triangle carrier. The triangular wave generator emits a sync pulse at zero value for timing control of the entire controller. At the maximum value, the voltage command of the current controller is compared with the counter to generate a PWM waveform.

The signal timing relationship of the entire module is shown in Fig. 7.

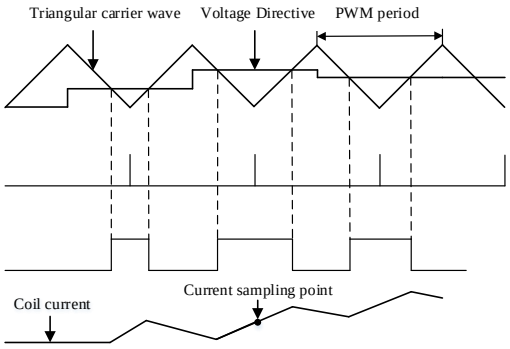

Figure 7. The timing diagram of PWM circuits

B. *Timing planning*

All control sequences of the control system are based on the synchronization pulse, and various control signals are generated by the timing controller. The frequency of the synchronization pulse is equal to the current loop sampling frequency is 20 KHz, and each synchronization pulse will start the current loop calculation. The sampling frequency of the displacement loop is 6.67 KHZ, and three sync pulses initiate a displacement loop calculation.

VI. PERFORMANCE TESTING AND RESULTS

The controller performance test is conducted based on the national university of defense technology independently developed MSCMG prototype system. The details of the control and power amplifier circuit board are shown in Fig. 8. On the right is the amplifier circuit board and on the left is the control circuit board.

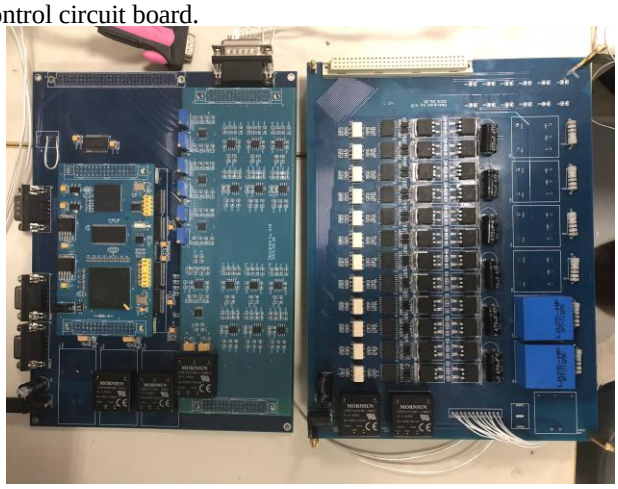

Figure 8. The control circuit board and power amplifier circuit board

Fig. 9 shows the control effect of the controller when MSCMG is still suspended. Where, x, y, tx and ty are radial displacement and around radial displacement respectively. The rotor displacement is controlled within the range of 5um, and the rotor is suspended with high precision.

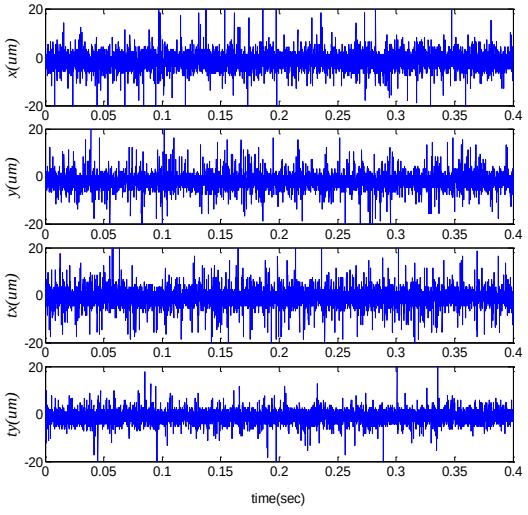

Figure 9. Experimental test results of 4-channel in case of no speed suspension

Fig. 10 shows the rotor speed at 3000rpm/min, the radial displacement of rotor is reduced from 15um to 10um by applying active vibration control algorithm.

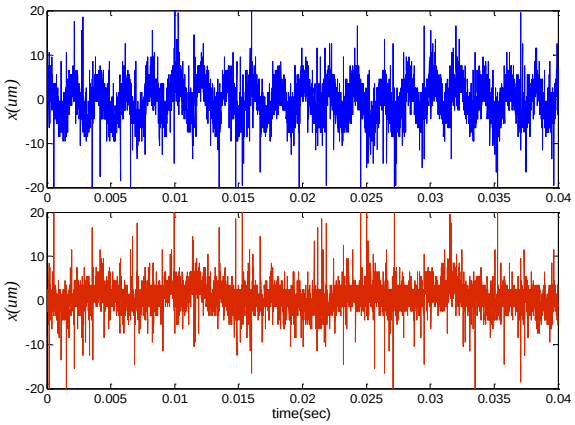

Figure 10. Experimental test results of X-channel before and after active vibration control taken in case of constant rotational speed 3000r/min

The experimental results show that the controller can achieve high accuracy, high stability and low power dissipation suspension of MSCMG.

VII. CONCLUSION

This article describes a six-channel and five-freedom magnetic bearing controller for MSCMG based on DSP and FPGA.

The highlight of this paper is to make full use of the computation ability of DSP and the flexible interface of FPGA. The designed controller can achieve the suspension control and active vibration control of the MSCMG simultaneously. Experiment results show that the maximum radial position error at the rotation speeds of 3000 rpm /min is less than 10um (less than 5% of the protection gap) based on the MSCMG prototype system.

REFERENCES

[1] Peng C, Fang J, Xu S. “Composite anti-disturbance controller for magnetically suspended control moment gyro subject to mismatched disturbances”. *Nonlinear Dynamics*, vol. 79, no. 2, pp. 1563-1573,2015.

[2] Zheng S, Yang J, Song X, et al. “Nutation Mode Tracking Compensation Control for High-speed Rotors With Gyroscopic Effects in Control Moment Gyros”. *IEEE Transactions on Industrial Electronics*, vol. 65, no. 5, pp. 4156-4165, 2017.

[3] S. P. Bhat, P. K. Tiwari. “Controllability of spacecraft attitude using control moment gyroscopes,” *IEEE Transactions on Automatic Control*, vol. 50, no. 3, pp. 585–590, 2009.

[4] Fang Jiancheng and Ren yuan. “High-precision control for a single-gimbal magnetically suspended control moment gyro based on inverse system method,” *IEEE Trans. Industrical Electronics*, vol. 58, no. 9, pp. 4331–4342, 2011.

[5] Peng C, Fang J, Xu X. “Mismatched Disturbance Rejection Control for Voltage-Controlled Active Magnetic Bearing via State-Space Disturbance Observer”. *IEEE Transactions on Power Electronics*, vol. 30, no. 5, pp. 2753-2762, 2015.

[6] Monmasson E, Cirstea M N. “FPGA Design Methodology for Industrial Control Systems—A Review,” *IEEE Transactions on Industrial Electronics*, vol. 54, no. 4, pp. 1824-1842, 2007.

[7] Liu B, Fang J, Liu G. “Implementation of active vibration control for magnetically suspended flywheels based on TMS320c6713B+FPGA digital controller”. *Optics and Precision Engineering*, vol. 17, no. 1, pp. 151-157, 2009.

[8] Zhang Li, Liu Kun. “Integrated control system design of magnetic bearings for flywheel based on FPGA,” *Electric Machines and Control*, vol. 16, no. 4, pp. 84-90, 2012.

[9] Zhang F, Li G, Liu G, et al. “Active and Passive Magnetic Suspension Flywheel Integrated Control Based on TMS320C31+FPGA Digital Controller”. *Journal of Engineering for Thermal Enercy and Power*, vol. 26, no. 6, pp. 756-759, 2011.